

Diffusion-weighted MRI in familial Creutzfeldt–Jakob disease with the codon 200 mutation in the prion protein gene

Yoshio Tsuboi^{a,*}, Yasuhiko Baba^b, Katsumi Doh-ura^c, Akiko Imamura^a,
Shinsuke Fujioka^a, Tatsuo Yamada^a

^aFifth Department of Internal Medicine, Fukuoka University School of Medicine, 7-45-1 Nanakuma, Johnan-ku, Fukuoka 814-0180, Japan

^bDepartment of Neurology, Mayo Clinic Jacksonville, Florida, USA

^cDepartment of Prion Research, Tohoku University, Sendai, Japan

Received 28 July 2004; received in revised form 11 January 2005; accepted 12 January 2005

Available online 25 February 2005

Abstract

Magnetic resonance imaging (MRI) with diffusion-weighted imaging (DWI) has been reported to be a useful tool for early diagnosis of sporadic Creutzfeldt–Jakob disease (CJD). We report MRI findings with DWI, as well as with fluid-attenuated inversion recovery (FLAIR) and T1-weighted imaging (T1WI), in a case of familial CJD with a mutation at codon 200 of the prion protein gene. DWI in this patient showed high signal intensity in the basal ganglia and the cerebral cortex, similar to findings in sporadic CJD. In addition, T1WI showed areas of high signal intensity bilaterally in the globus pallidus. Despite the clinical diversity and atypical laboratory findings seen in familial CJD with the codon 200 mutation, these neuroimaging studies suggest that common regional distributions and a common pathogenesis might underlie the clinical progression both in sporadic CJD and in familial CJD with the codon 200 mutation in the prion protein gene. DWI abnormalities may be characteristic features that should be considered in the diagnosis of familial as well as of sporadic CJD.

© 2005 Elsevier B.V. All rights reserved.

Keywords: Creutzfeldt–Jakob disease; Diagnostic methods; Diffusion-weighted imaging; Familial; Magnetic resonance imaging; Prion disease; Prion gene mutation

1. Introduction

Creutzfeldt–Jakob disease (CJD) is a rare and fatal neurodegenerative disorder caused by abnormal prion protein accumulation in the brain [1–3]. CJD may occur in sporadic, infectious, or familial forms. The familial form is found in 10% to 15% of all cases of CJD [4]. The diagnosis of CJD is usually based on clinical features, characteristic electroencephalographic (EEG) activity, and laboratory values. The clinical features consist of rapidly progressive dementia, myoclonus, and ataxia and are typically fatal within 1 year from the onset of symptoms

[1–3]. EEG activity in CJD is characterized by periodic sharp and slow wave complexes [5]. Laboratory criteria include an elevated concentration of neuron-specific enolase (NSE) and the presence of 14–3–3 protein in the cerebrospinal fluid (CSF) [5–8].

Diagnosis of familial CJD is often difficult because clinical presentation varies widely, and characteristic features are not always present [6,9]. Familial CJD can be caused by several different mutations in the prion protein gene [4]. Atypical clinical features may be related to different genotypes at codon 129 or 219 [10,11]. One mutation at codon 200 in the prion protein gene is known to present with diverse clinical characteristics ranging from features similar to those of sporadic CJD [12–15] to atypical features such as slow progression of symptoms, fatal insomnia, polyneuropathy, lack of characteristic EEG

* Corresponding author. Tel.: +81 92 801 1011; fax: +81 92 865 7900.
E-mail address: tsuboi@cis.fukuoka-u.ac.jp (Y. Tsuboi).

abnormalities, and absence of 14–3–3 protein in the CSF [10,16,17].

Thus, a useful diagnostic tool is needed, particularly for patients without a known family history of CJD. The presence of 14–3–3 protein in the CSF has been recognized to have good sensitivity and specificity as an indicator of sporadic CJD [5–7,18]. However, no studies have been published on the sensitivity and specificity of CSF abnormalities in familial CJD, and as many as 25% of patients with familial CJD may have normal 14–3–3 protein and NSE concentrations in the CSF [5,6].

Magnetic resonance imaging (MRI) has been reported to be a useful tool for early diagnosis of sporadic CJD. For example, MRI with diffusion-weighted images (DWI) shows increased signals in the basal ganglia and cerebral cortex of patients with sporadic CJD [19–28]. Whether MRI is equally useful in the diagnosis of familial CJD remains unclear, although several MRI studies have been reported in familial CJD with various mutations in the prion protein gene [29–32].

To further investigate whether MRI might be useful in the diagnosis of familial CJD, we examined the brain of a patient with familial CJD in whom the codon 200 mutation was confirmed by molecular genetic analysis. DWI, fluid-attenuated inversion recovery (FLAIR) imaging, and T1-weighted imaging (T1WI) were performed, and the results were compared with findings in the literature on patients with sporadic CJD.

2. Case report

2.1. Clinical description

A 64-year-old right-handed woman born in southern Japan was admitted to our hospital because of forgetfulness, dysarthria, and impaired balance. She had noticed the forgetfulness and insomnia 3 months before admission. Fatigue, motor slowness, and dysarthria had developed 2 months before admission. The frequency of spontaneous speech had gradually decreased, and she had increasingly experienced loss of balance, leading to falls. The patient's mother died at age 55 of a progressive dementing disorder, and her younger sister had received a diagnosis of familial CJD at another hospital.

At admission to our hospital, the patient was alert and cooperative, but inattentive. She was able to follow simple commands, and her Mini-Mental State Examination (MMSE) score at that time was 23 of 30 possible points. Her speech was slurred, and scanning speech was occasionally evident. Her pupils were normal in size and reacted to light stimulation. Extraocular movement was normal. Cerebellar ataxia was detected, including dysmetria and decomposition in all extremities. Her gait was also ataxic and wide based. No involuntary movements were observed. She did not smoke or consume alcohol and had no history of toxic exposure. Results of extensive laboratory evaluations of serum, urine, and CSF were normal, except for positive

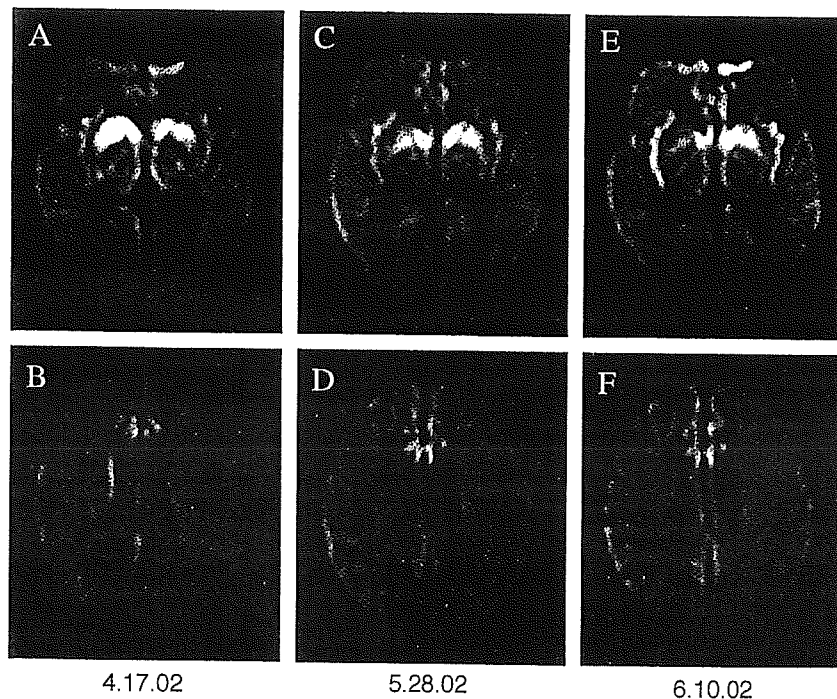


Fig. 1. Magnetic resonance imaging of the brain of a patient with familial Creutzfeldt–Jakob disease, performed with serial diffusion-weighted images (DWI). (A) and (B) were performed at admission to hospital, (C) and (D) at approximately 1 month, and (E) and (F) at 2 months after admission. (A) and (B) High signal intensity bilaterally in the basal ganglia, insula, and cingulate gyrus. (C) and (D) Slightly decreased hyperintense bilateral signals in the basal ganglia; extension of signals in the cortex into left temporoparietal cortex and cingulate gyrus. (C) Increased signal intensity in areas of hyperintensity in insular cortex. (E) and (F) Slight decrease in hyperintense signals in cingulate gyrus, insular cortex, left temporoparietal cortex, and basal ganglia.

14–3–3 protein (+; normal, negative) and elevated NSE (77 ng/mL; normal, <35 ng/mL) in the CSF. At that time, EEG showed diffuse slow waves without periodic sharp waves.

A diagnosis of familial CJD was made, and treatment with quinacrine was started at 300 mg/day. Despite treatment, the patient's speech and gait deteriorated rapidly. Her cognitive decline also progressed rapidly in association with myoclonic jerks in the upper extremities. Subsequently, both spontaneous and stimulus-induced episodes of myoclonus were seen in all extremities. Rigidity, Babinski signs, snout reflex, and bilateral grasping reflex also developed. One month after admission (4 months after the onset of symptoms), EEG showed diffuse slow and periodic sharp-wave complex discharges.

Genomic DNA was extracted from peripheral lymphocytes. The coding sequence of the prion protein gene was amplified by using polymerase chain reaction. Genetic study confirmed the point mutation at codon 200 (GAG→AAG) resulting in the substitution of lysine for glutamate.

2.2. Magnetic resonance imaging studies

MRI of the brain was performed with DWI, FLAIR imaging, and T1WI at admission, as well as approximately 1 and 2 months later.

At admission, DWI demonstrated high signal intensity bilaterally in the basal ganglia, insula, and cingulate gyrus

(Fig. 1A and B). FLAIR imaging also showed high signal intensity bilaterally in the basal ganglia (Fig. 2A). Apparent diffusion coefficient (ADC) mapping of these regions revealed decreased signal intensity, indicating cytotoxic edema. T1-weighted imaging (T1WI) showed normal results (Fig. 2B).

DWI performed approximately 1 month after admission showed that the hyperintense signals in the basal ganglia had decreased slightly and those in the cortex had extended into the left temporoparietal cortex and the cingulate gyrus (Fig. 1C and D). DWI also showed that the hyperintensity in the insular cortex had increased in signal intensity (Fig. 1C). On T1WI, spotty hyperintense signals had appeared bilaterally in the globus pallidus (Fig. 2D).

On DWI performed 2 months after admission, the degree of hyperintensity in regions involving the cingulate gyrus, insular cortex, left temporoparietal cortex, and basal ganglia had decreased slightly (Fig. 1E and F). On T1WI, the increased signal intensity in the globus pallidus was more apparent than it had been 1 month after admission (Fig. 2F).

3. Discussion

The case we describe helps to clarify the role of MRI as a diagnostic tool in patients with familial CJD. Familial CJD with the codon 200 mutation was confirmed by genetic

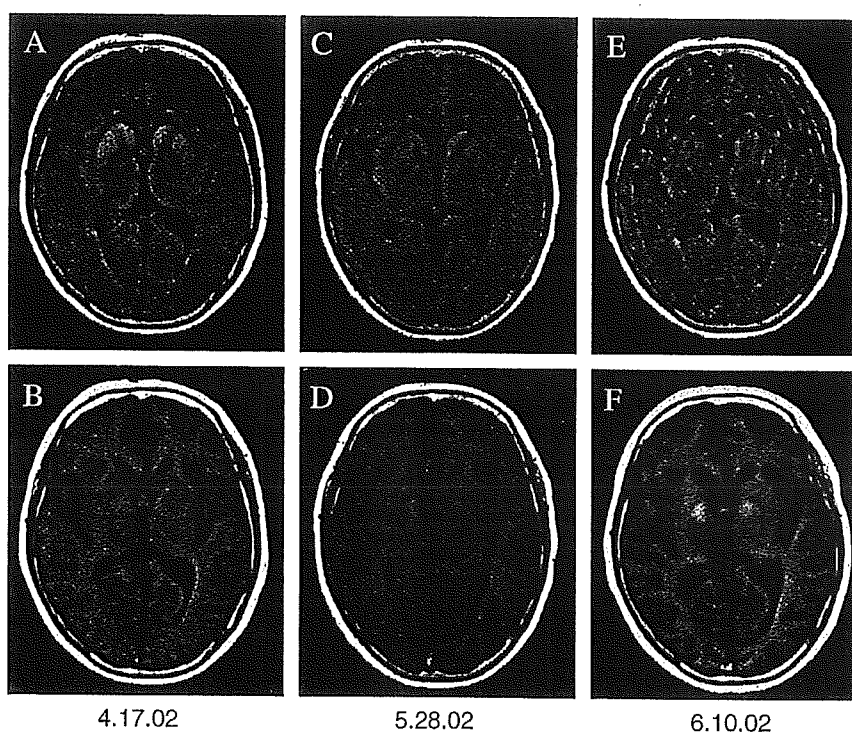


Fig. 2. Magnetic resonance imaging of the brain with serial fluid-attenuated inversion recovery (FLAIR) and T1-weighted imaging (T1WI). (A) and (B) were performed at admission, (C) and (D) at approximately 1 month, and (E) and (F) at 2 months after admission. (A) Hyperintense signals in the bilateral basal ganglia on FLAIR image. (B) Normal T1WI. (C) Slightly decreased hyperintense signals in the bilateral basal ganglia on FLAIR image. (D) Bilateral spotty hyperintense signals in the globus pallidus on T1WI. (E) No significant signal change in FLAIR (compared with FLAIR image at 1 month), but artifact prevented precise evaluation. (F) Increased signal intensity in the globus pallidus on T1WI (more apparent than at 1 month).

study in our patient. As has also been reported for other patients with this mutation [10,12–17], progression was more aggressive in our patient than in those with sporadic CJD. However, most clinical features of our case were similar to those of sporadic CJD, including rapidly progressive ataxia, severe mental deterioration, myoclonus, and typical periodic sharp-wave activity on EEG approximately 4 months after the onset of symptoms.

DWI abnormalities in our patient were observed as areas of high signal intensity in the putamen and caudate nucleus and as ribbon-like areas of hyperintensity in the cortical areas, predominantly in the insula, cingulate gyrus, and temporoparietal lobe. Although corresponding FLAIR images showed some hyperintensity in the basal ganglia, ADC mapping performed at the same time showed reduced signals in the corresponding regions, indicating that T2 shine-through contributed to the hyperintensity in the DWI only to a slight degree. The abnormalities found in our patient resemble those observed in sporadic CJD [19–28], demonstrating that similar MRI abnormalities can be found in both forms of the disease.

DWI appears to be a valuable tool that should be included in the diagnostic criteria for CJD [33]. Marked DWI changes can be observed in the early stages of symptomatic onset and are sustained over several months, although the high signal intensity seen on DWI may disappear over time in patients with advanced sporadic CJD (unpublished data). Shiga et al. [33] concluded that DWI was a more sensitive test for the early clinical diagnosis of CJD than periodic sharp wave complexes on EEG, detection of CSF 14–3–3 protein, or increase of NSE in the CSF. DWI may detect areas of increased signal intensity in the basal ganglia and cerebral cortex with greater sensitivity than that of routine MRI sequences such as T1WI, T2WI, or FLAIR images [18,34].

The pathogenesis of DWI abnormalities in the basal ganglia and cerebral cortex in CJD is not well understood. Spongiform neuronal degeneration and microglial activation might contribute to the changes demonstrated on DWI [35,36]. Cambier et al. [37] have suggested that high signal intensity on DWI may be related to periodic sharp-wave complex discharges on EEG. The EEG did not show specific changes corresponding to the DWI abnormalities in our case. Although our patient showed positive 14–3–3 protein and increased NSE in the CSF, as in sporadic CJD, it is unclear whether these findings are also related to the DWI abnormalities.

T1WI signals in the globus pallidus were initially normal in our patient and increased in intensity bilaterally during the early stages. This phenomenon might represent rapid pathologic changes in the basal ganglia during the course of the illness, corresponding to the hyperintensities shown on DWI. Such changes have previously been reported in only 1 patient with sporadic CJD, who showed typical clinical characteristics [38]. Although the high T1WI signal intensity in the globus pallidus may have been due to

accumulation of prion protein in the brain [38], increased metal concentration can also cause high signal intensity on T1WI [39]. It remains doubtful whether T1WI abnormalities are pathognomonic for either sporadic or familial CJD.

To our knowledge, this is the first report to of MRI showing DWI and T1WI abnormalities in familial CJD with a point mutation at codon 200. Despite the clinical diversity and atypical laboratory findings seen in familial CJD with the codon 200 mutation, these neuroimaging studies suggest that common regional distributions and a common pathogenesis might underlie the clinical progression in both sporadic and familial CJD with the codon 200 mutation in the prion protein gene. Thus, DWI abnormalities may be characteristic features that should be considered in the diagnosis of familial as well as of sporadic CJD.

References

- [1] Brown P, Cathala F, Castaigne P, Gajdusek DC. Creutzfeldt–Jakob disease: clinical analysis of a consecutive series of 230 neuropathologically verified cases. *Ann Neurol* 1986;20:597–602.
- [2] Johnson RT, Gibbs CJ. Creutzfeldt–Jakob disease and related transmissible spongiform encephalopathies. *N Engl J Med* 1998;339:1994–2004.
- [3] Richardson EP, Masters CL. The nosology of Creutzfeldt–Jakob disease and conditions related to the accumulation of PrP^{CJD} in the nervous system. *Brain Pathol* 1995;5:33–41.
- [4] Masters CL, Harris JO, Gajdusek DC, Gibbs Jr CJ, Bernoulli C, Asher DM. Creutzfeldt–Jakob disease: patterns of worldwide occurrence and the significance of familial and sporadic clustering. *Ann Neurol* 1979;5:177–88.
- [5] Zerr I, Pocchiari M, Collins S, Brandel JP, de Pedro Cuesta J, Knight RS, et al. Analysis of EEG and CSF 14–3–3 proteins as aids to the diagnosis of Creutzfeldt–Jakob disease. *Neurology* 2000;55:811–5.
- [6] Zerr I, Bodemer M, Gefeller O, Otto M, Poser S, Wiltfang J, et al. Detection of 14–3–3 protein in the cerebrospinal fluid supports the diagnosis of Creutzfeldt–Jakob disease. *Ann Neurol* 1998;43:32–40.
- [7] Hsich G, Kenney K, Gibbs CJ, Lee KH, Harrington MG. The 14–3–3 brain protein in cerebrospinal fluid as a marker for transmissible spongiform encephalopathies. *N Engl J Med* 1996;335:924–30.
- [8] Aksamit Jr AJ, Preissner CM, Homburger HA. Quantitation of 14–3–3 and neuron-specific enolase proteins in CSF in Creutzfeldt–Jakob disease. *Neurology* 2001;57:728–30.
- [9] Brandel JP, Delasnerie-Laupretre N, Laplanche JL, Hauw JJ, Alperovitch A. Diagnosis of Creutzfeldt–Jakob disease: effect of clinical criteria on incidence estimates. *Neurology* 2000;54:1095–9.
- [10] Seno H, Tashiro H, Ishino H, Inagaki T, Nagasaki M, Morikawa S. New haplotype of familial Creutzfeldt–Jakob disease with a codon 200 mutation and a codon 219 polymorphism of the prion protein gene in a Japanese family. *Acta Neuropathol (Berl)* 2000;99:125–30.
- [11] Hauw JJ, Sazdovitch V, Laplanche JL, Peoc'h K, Kopp N, Kemeny J, et al. Neuropathologic variants of sporadic Creutzfeldt–Jakob disease and codon 129 of PrP gene. *Neurology* 2000;54:1641–6.
- [12] Meiner Z, Gabizon R, Prusiner SB. Familial Creutzfeldt–Jakob disease. Codon 200 prion disease in Libyan Jews. *Medicine (Baltimore)* 1997;76:227–37.
- [13] Iwabuchi K, Endoh S, Hagimoto H, Okamoto K, Miyakawa T, Yamaguchi T, et al. Three patients from two families with familial Creutzfeldt–Jakob disease having a point mutation in the prion protein gene at codon 200 (Glu→Lys). *No To Shinkei* 1994;46:349–54.
- [14] Kawauchi Y, Okada M, Kuroiwa Y, Ishihara O, Akai J. Familial Creutzfeldt–Jakob disease with the heterozygous point mutation at

- codon 200 of the prion protein gene (Glu→Lys)—report of CJD200 brothers of Yamanashi Prefecture origin. *No To Shinkei* 1997;49:460–4.
- [15] Salvatore M, Pocchiari M, Cardone F, Petraroli R, D'Alessandro M, Galvez S, et al. Codon 200 mutation in a new family of Chilean origin with Creutzfeldt–Jakob disease. *J Neurol Neurosurg Psychiatry* 1996;61:111–2.
- [16] Chapman J, Arlazoroff A, Goldfarb LG, Cervenakova L, Neufeld MY, Werber E, et al. Fatal insomnia in a case of familial Creutzfeldt–Jakob disease with the codon 200 (Lys) mutation. *Neurology* 1996;46:758–61.
- [17] Antoine JC, Laplanche JL, Mosnier JF, Beaudry P, Chatelain J, Michel D. Demyelinating peripheral neuropathy with Creutzfeldt–Jakob disease and mutation at codon 200 of the prion protein gene. *Neurology* 1996;46:1123–7.
- [18] Mendez OE, Shang J, Jungreis CA, Kaufer DI. Diffusion-weighted MRI in Creutzfeldt–Jakob disease: a better diagnostic marker than CSF protein 14–3–3? *J Neuroimaging* 2003;13:147–51.
- [19] Bahn MM, Kido DK, Lin W, Pearlman AL. Brain magnetic resonance diffusion abnormalities in Creutzfeldt–Jakob disease. *Arch Neurol* 1997;54:1411–5.
- [20] Bahn MM, Parchi P. Abnormal diffusion-weighted magnetic resonance images in Creutzfeldt–Jakob disease. *Arch Neurol* 1999;56:577–83.
- [21] Demaerel P, Baert AL, Vanopdenbosch L, Robberecht W, Dom R. Diffusion-weighted magnetic resonance imaging in Creutzfeldt–Jakob disease. *Lancet* 1997;349:847–8.
- [22] Demaerel P, Heiner L, Robberecht W, Sciot R, Wilms G. Diffusion-weighted MRI in sporadic Creutzfeldt–Jakob disease. *Neurology* 1999;52:205–8.
- [23] Demaerel P, Sciot R, Robberecht W, Dom R, Vandermeulen D, Maes F, et al. Accuracy of diffusion-weighted MR imaging in the diagnosis of sporadic Creutzfeldt–Jakob disease. *J Neurol* 2003;250:222–5.
- [24] Matoba M, Tonami H, Miyaji H, Yokota H, Yamamoto I. Creutzfeldt–Jakob disease: serial changes on diffusion-weighted MRI. *J Comput Assist Tomogr* 2001;25:274–7.
- [25] Na DL, Suh CK, Choi SH, Moon HS, Seo DW, Kim SE, et al. Diffusion-weighted magnetic resonance imaging in probable Creutzfeldt–Jakob disease: a clinical–anatomic correlation. *Arch Neurol* 1999;56:951–7.
- [26] Nagaoka U, Kurita K, Hosoya T, Kitamoto T, Kato T. Diffusion images on brain MRI in Creutzfeldt–Jakob disease. *Clin Neurol* 1999;39:468–70.
- [27] Schaefer PW, Grant PE, Gonzalez RG. Diffusion-weighted MR imaging of the brain. *Radiology* 2000;217:331–45.
- [28] Yee AS, Simon JH, Anderson CA, Sze CI, Filley CM. Diffusion-weighted MRI of right-hemisphere dysfunction in Creutzfeldt–Jakob disease. *Neurology* 1999;52:1514–5.
- [29] Nitrini R, Mendonca RA, Huang N, LeBlanc A, Livramento JA, Marie SK. Diffusion-weighted MRI in two cases of familial Creutzfeldt–Jakob disease. *J Neurol Sci* 2001;184:163–7.
- [30] Ishida S, Sugino M, Koizumi N, Shinoda K, Ohsawa N, Ohta T, et al. Serial MRI in early Creutzfeldt–Jakob disease with a point mutation of prion protein at codon 180. *Neuroradiology* 1995;37:531–4.
- [31] Huang N, Marie SK, Kok F, Nitrini R. Familial Creutzfeldt–Jakob disease associated with a point mutation at codon 210 of the prion protein gene. *Arq Neuropsiquiatr* 2001;59:932–5.
- [32] Satoh A, Goto H, Satoh H, Tomita I, Seto M, Furukawa H, et al. A case of Creutzfeldt–Jakob disease with a point mutation at codon 232: correlation of MRI and neurologic findings. *Neurology* 1997;49:1469–70.
- [33] Shiga Y, Miyazawa K, Sato S, Fukushima R, Shibuya S, Sato Y, et al. Diffusion-weighted MRI abnormalities as an early diagnostic marker for Creutzfeldt–Jakob disease. *Neurology* 2004;64:443–9.
- [34] Mendez OE, Shang J, Jungreis CA, Kaufer DI. Accuracy of diffusion-weighted MR imaging in the diagnosis of sporadic Creutzfeldt–Jakob disease. *J Neurol* 2003;250:222–5.
- [35] Bergui M, Bradac GB, Rossi G, Orsi L. Extensive cortical damage in a case of Creutzfeldt–Jakob disease: clinico-radiological correlations. *Neuroradiology* 2003;45:304–7.
- [36] Mittal S, Farmer P, Kalina P, Kingsley PB, Halperin J. Correlation of diffusion-weighted magnetic resonance imaging with neuropathology in Creutzfeldt–Jakob disease. *Arch Neurol* 2002;59:128–34.
- [37] Cambier DM, Kantarci K, Worrell GA, Westmoreland BF, Aksamit AJ. Lateralized and focal clinical, EEG, and FLAIR MRI abnormalities in Creutzfeldt–Jakob disease. *Clin Neurophysiol* 2003;114:1724–8.
- [38] de Priester JA, Jansen GH, de Kruijk JR, Wilmink JT. New MRI findings in Creutzfeldt–Jakob disease: high signal in the globus pallidus on T1-weighted images. *Neuroradiology* 1999;41:265–8.
- [39] Maeda H, Sato M, Yoshikawa A, Kimura M, Sonomura T, Terada M, et al. Brain MR imaging in patients with hepatic cirrhosis: relationship between high intensity signal in basal ganglia on T1-weighted images and elemental concentrations in brain. *Neuroradiology* 1997;39:546–50.



ELSEVIER



www.elsevierhealth.com/journals/jinf

Cerebroventricular infusion of pentosan polysulphate in human variant Creutzfeldt-Jakob disease

N.V. Todd^a, J. Morrow^b, K. Doh-ura^c, S. Dealler^d, S. O'Hare^e, P. Farling^f, M. Duddy^b, N.G. Rainov^{g,*}

^aRegional Neurosciences Centre, Newcastle General Hospital NHS Trust, Newcastle, UK

^bDepartment of Neurology, Royal Victoria Hospital, Belfast, UK

^cDepartment of Prion Research, Tohoku University Graduate School of Medicine, Japan

^dDepartment of Microbiology, Lancaster General Infirmary; Lancaster, UK

^eDepartment of Pharmacy, Royal Victoria Hospital, Belfast, UK

^fDepartment of Anesthetics, Royal Victoria Hospital, Belfast, UK

^gDepartment of Neurological Science, The University of Liverpool, and The Walton Centre for Neurology and Neurosurgery NHS Trust, Lower Lane, Liverpool L9 7LJ, UK

Accepted 24 July 2004

Available online 22 September 2004

KEYWORDS

Brain;
Intraventricular;
New variant CJD;
Pentosan polysulphate

Abstract Variant Creutzfeldt-Jakob disease (CJD) is a transmissible spongiform encephalopathy believed to be caused by the bovine spongiform encephalopathy agent, an abnormal isoform of the prion protein (PrP^{Sc}). At present there is no specific or effective treatment available for any form of CJD. Pentosan polysulphate (PPS), a large polyglycoside molecule with weak heparin-like activity, has been shown to prolong the incubation period of the intracerebral infection when administered to the cerebral ventricles in a rodent scrapie model. PPS also prevents the production of further PrP^{Sc} in cell culture models.

These properties of PPS prompted its cerebroventricular administration in a young man with vCJD. Long-term continuous infusion of PPS at a dose of 11 µg/kg/day for 18 months did not cause drug-related side effects. Follow-up CT scans demonstrated progressive brain atrophy during PPS administration. Further basic and clinical research is needed in order to address the issue of efficacy of PPS in vCJD and in other prion diseases.

© 2004 The British Infection Society. Published by Elsevier Ltd. All rights reserved.

Introduction

Variant Creutzfeldt-Jakob disease (vCJD) is a form of CJD believed to be caused by the bovine spongiform encephalopathy agent.¹⁻³ Unlike the

* Corresponding author. Tel.: +44-151-529-5323; fax: +44-151-529-5465.

E-mail address: rainov@liv.ac.uk (N.G. Rainov).

sporadic form, vCJD mostly becomes symptomatic in young adults and adolescents.¹ Pentosan polysulphate (PPS) is a large polyglycoside molecule with weak heparin-like activity. It has been shown to prevent the propagation of the abnormal isoform of the prion protein (PrP^{Sc}) in cell culture models,⁴ and to prolong the incubation period of intracerebral infection in rodent scrapie models when administered either systemically⁵ or directly into the cerebral ventricles.⁶ These properties of PPS prompted our use of cerebroventricular PPS in escalating doses in one patient with vCJD to assess the safety and tolerability of the drug when administered by this route.

Case report and discussion

The patient is a 20-year-old man who presented initially at the age of 16 years and 11 months with subjective signs of behavioural disturbance. A few months later this was followed by progressive ataxia, pyramidal signs and myoclonus, which led to the clinical diagnosis of possible vCJD. The clinical picture combined with abnormal MR findings in the FLAIR sequence (pulvinar sign) and positive tonsil biopsy allowed the diagnosis of probable vCJD 8 months after the initial clinical symptoms (Fig. 1). At the time of initial administration of PPS (Pentosan polysulphate SP54, Bene Arzneimittel GmbH, Munich, Germany) into the cerebral ventricular system, the patient had symptoms of advanced vCJD,⁷ such as ataxia, dementia, dysphagia, dysphasia, myoclonus, and was confined to bed and unable to care for himself. He was fed via percutaneous gastrostomy.

A permanently implanted right frontal intraventricular catheter was connected to a subcutaneous

programmable pump (SynchroMed EL, Medtronic Inc.). The initial PPS dose of 1 µg/kg/d was escalated without significant problem to the target dose, extrapolated from animal studies, of 11 µg/kg/d. A possible therapeutic dose-effect relationship for intracerebroventricular PPS in humans with prion disease remains unknown, and therefore further dose escalation would only be limited by side effects. In mice, dose-response studies with PPS have shown that the most effective dose is 230 µg/kg/d.⁶ In our current human dosing this would translate to 23 µg/kg/d, which is a little more than twice the current daily dose of PPS.

Continuous infusion of PPS for 18 months did not cause any drug-related side effects. Cerebroventricular PPS at the above dose did not have any measurable systemic anticoagulant activity in serum, as confirmed by unchanged INR (international normalised ratio) before and during PPS infusion.

Follow-up CT scans demonstrated no intracerebral haemorrhage (Fig. 2), and there were no seizures. A right parietal subdural fluid collection of increasing size was noted on CT scans 8 months after start of PPS infusion and necessitated surgical (burr hole) evacuation of fluid. PPS infusion was halted temporarily and restarted one week after the surgery. Due to recurrent subdural fluid collections, two further surgical revisions were necessary.

Clearly comments on efficacy are difficult in the setting of a single case, but after 18 months of continuous cerebroventricular PPS administration, the patient is still alive and there is some evidence of a change in the neurological condition. He is now able to fix his eyes on persons, to obey simple one stage commands, and to make verbalization attempts in response to stimuli. The sleep/wake cycle and the reflex swallow are restored and the

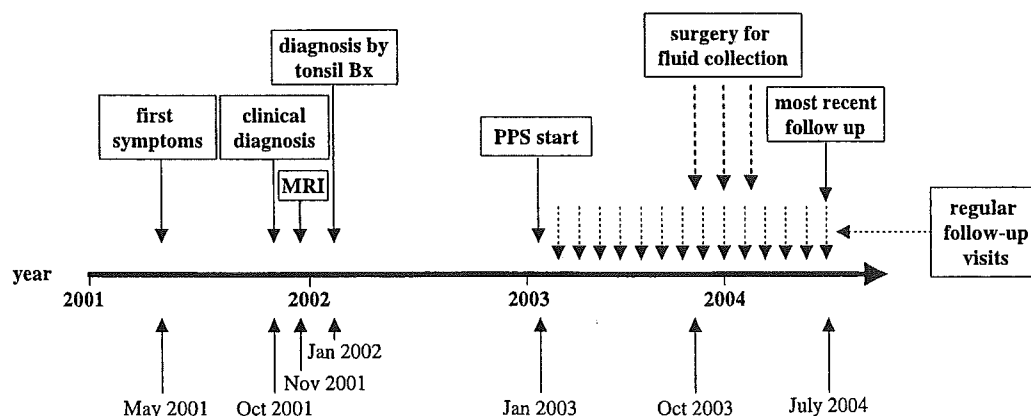


Figure 1 Schematic representation of the time course of disease presentation, diagnosis and management. Bx= biopsy.

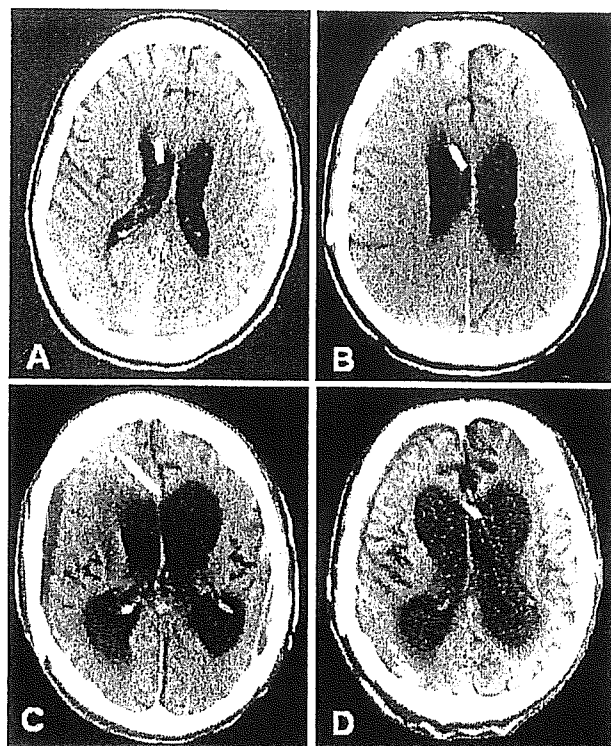


Figure 2 (A) Non-enhanced CT scan on day 6 after start of cerebroventricular PPS infusion. (B) Non-enhanced CT scan 3 months after start of PPS infusion. Note the slightly enlarged lateral ventricles compared to baseline (A). (C) Non-enhanced CT scan 1-year after start of PPS infusion. (D) Non-enhanced CT scan 15 months after start of PPS infusion. Note progressing cortical and subcortical atrophy with enlargement of the ventricular system on scans C and D.

myoclonus is reduced. The patient has gained 5 kg of weight compared to pre-PPS baseline, while on the same nutritional regime. Regular follow-up observations and pump refills (every 6 weeks) were carried out by the same medical and nursing staff and physiotherapists involved with the patient's care from the early stages of his disease. Despite the apparent trend towards clinical improvement, brain atrophy, as seen on regular follow-up CT scans, continued to progress during the period of PPS administration and resulted in ventriculomegaly and grossly enlarged extracerebral CSF spaces (Fig. 2).

In conclusion, cerebroventricular infusion of PPS at 11 $\mu\text{g}/\text{kg}/\text{d}$ appears safe and well tolerated for continuous long-term application. Our patient has survived for 37 months after initial symptoms and 30 months after diagnosis of probable vCJD, while the median duration of illness with vCJD is 13 months (range 6-39)⁷.

Further lessons have also been learned from this first case. Firstly, surgery in a brain affected by

vCJD may result in a higher rate of surgical complications than might be expected in a normal patient. We suggest that in order to allow the catheter track to organise, drug infusion should be delayed for at least 7-10 days after implantation of the pump system. Regular neuroradiological follow-up throughout the treatment period is strongly recommended. Secondly, if clinically significant benefits are to be expected, PPS administration should start as early as possible in the course of the disease and before irreversible loss of neurological function has occurred.

Further clinical, neuroradiological and laboratory investigations in the setting of a prospective clinical study with standardised follow-up protocol and data collection are essential in order to assess the efficacy of PPS administration in vCJD and in other prion diseases.

Acknowledgements

The authors would like to thank Dr R. Knight (Edinburgh) and Dr C. Pomfrett (Manchester) for useful comments and suggestions regarding the manuscript. Dr M. McClean (Belfast) is gratefully acknowledged for his general medical input and practical support.

References

1. Will RG, Ironside JW, Zeidler M, Cousens SN, Estibeiro K, Alperovitch A, Poser S, Pocchiari M, Hofman A, Smith PG. A new variant of Creutzfeldt-Jakob disease in the UK. *Lancet* 1996;347:921-5.
2. Bruce ME, Will RG, Ironside JW, McConnell I, Drummond D, Suttie A, McCordle L, Chree A, Hope J, Birkett C, Cousens S, Fraser H, Bostock CJ. Transmissions to mice indicate that 'new variant' CJD is caused by the BSE agent. *Nature* 1997;389:498-501.
3. Hill AF, Desbruslais M, Joiner S, Sidle KC, Gowland I, Collinge J, Doey LJ, Lantos P. The same prion strain causes vCJD and BSE. *Nature* 1997;389:448-50.
4. Caughey B, Raymond GJ. Sulfated polyanion inhibition of scrapie-associated PrP accumulation in cultured cells. *J Virol* 1993;67:643-50.
5. Ladogana A, Casaccia P, Ingrosso L, Cibati M, Salvatore M, Xi YG, Masullo C, Pocchiari M. Sulphate polyanions prolong the incubation period of scrapie infected hamsters. *J Gen Virol* 1992;73:661-5.
6. Doh-ura K, Ishikawa K, Murakami-Kubo I, Sasaki K, Mohri S, Race R, Iwaki T. Treatment of transmissible spongiform encephalopathy by intraventricular drug infusion in animal models. *J Virol* 2004;78:4999-5006.
7. Henry C, Knight R. Clinical features of variant Creutzfeldt-Jakob disease. *Rev Med Virol* 2002;12:143-50.

Fatal familial insomnia with an unusual prion protein deposition pattern: an autopsy report with an experimental transmission study

K. Sasaki*, K. Doh-ura*, Y. Wakisaka*, H. Tomoda† and T. Iwaki*

*Department of Neuropathology, Neurological Institute, Graduate School of Medical Sciences, Kyushu University, Fukuoka, and †Department of Neurology, Imazu Red Cross Hospital, Imazu, Fukuoka, Japan

K. Sasaki, K. Doh-ura, Y. Wakisaka, H. Tomoda and T. Iwaki (2005) *Neuropathology and Applied Neurobiology* 31, 80–87

Fatal familial insomnia with an unusual prion protein deposition pattern: an autopsy report with an experimental transmission study

We recently performed a *post-mortem* examination on a Japanese patient who had a prion protein gene mutation responsible for fatal familial insomnia (FFI). The patient initially developed cerebellar ataxia, but finally demonstrated insomnia, hyperkinetic delirium, autonomic signs and myoclonus in the late stage of the illness. Histological examination revealed marked neuronal loss in the thalamus and inferior olivary nucleus; however, prion protein (PrP) deposition was not proved in these lesions by immunohistochemistry. Instead, PrP deposition and spongiform change were both conspicuous within the cerebral cortex, whereas particular PrP deposition was also observed within the cerebellar cortex. The abnormal protease-resistant PrP (PrP^{res}) molecules in the cerebral cor-

tex of this case revealed PrP^{res} type 2 pattern and were compatible with those of FFI cases, but the transmission study demonstrated that a pathogen in this case was different from that in a case with classical FFI. By inoculation with homogenate made from the cerebral cortex, the disease was transmitted to mice, and neuropathological features that were distinguishable from those previously reported were noted. These findings indicate the possibility that a discrete pathogen was involved in the disease in this case. We suggest that not only the genotype of the PrP gene and some other as yet unknown genetic factors, but also the variation in pathogen strains might be responsible for the varying clinical and pathological features of this disease.

Keywords: Creutzfeldt-Jakob disease, NZW mouse, prion disease, thalamic form, transmissible spongiform encephalopathy

Introduction

Fatal familial insomnia (FFI) is one of the disease entities of prion disease or transmissible spongiform encephalopathy (TSE) and it is linked to a mutation at codon 178 of the prion protein gene (PRNP), aspartic acid to asparagine substitution (D178N), in conjunction with methionine at the polymorphic position 129 of the mutant allele [1]. The

neuropathological hallmark of FFI is the predominance of lesions within the thalamus [2]. Clinically this disorder is characterized by progressive insomnia, dysautonomia and motor signs [3]. The D178N mutation is also associated with familial Creutzfeldt-Jakob disease (CJD). The disease phenotypes have been considered to depend on the polymorphism at codon 129 of the mutant allele, methionine (129Met) in FFI and valine (129Val) in CJD [4]. However, the FFI genotype reveals diverse clinical expression including cerebellar ataxia, dementia and autonomic abnormalities with or without insomnia [5,6]. In Japan, one FFI case [7] and some cases of the 'sporadic'

Correspondence: Kensuke Sasaki, Department of Neuropathology, Neurological Institute, Graduate School of Medical Sciences, Kyushu University, Fukuoka 812-8582, Japan. Tel: +81-92-6425539; Fax: +81-92-6425540; E-mail: ksasaki@np.med.kyushu-u.ac.jp

thalamic form of CJD [8,9] have been reported, and these have indicated a discrepancy between PRNP genotype and the disease phenotype.

We recently performed a *post-mortem* examination on a Japanese patient with a 27-month history of familial prion disease with PRNP D178N-129Met mutation. The clinical data on this patient and his family have been published in part [10]. Here we report additional clinical data and *post-mortem* neuropathological findings, as well as findings in mice infected with the patient's material.

Case report

The pedigree is presented in Figure 1. In October 1997, a 50-year-old Japanese man (Patient II-5) developed an unsteady gait, followed within a month by difficulty in speech. Although these symptoms worsened rapidly, he did not immediately develop either dementia or insomnia. He was admitted to a hospital for neurological evaluation in February 1998, and PRNP D178N-129Met mutation (heterozygous for 129Met/Val) was revealed as previously reported [10]. From October 1998, either insomnia or delirium was clearly apparent. Hyperthermia without any signs indicative of infection or inflammation, thus suggesting an autonomic sign, was also observed. He often showed reality disturbance and restlessness. He became progressively demented, developed trismus, myoclonus and horizontal nystagmus, and demonstrated increased muscle tone. Finally he became bedridden with flexion contracture. Brain computed tomography revealed mild atrophy of the cerebellum and brainstem. Electroencephalograms showed a background of 9 Hz diffuse α activities, but periodic synchronous discharges were not

detected during the clinical course. Sleep activities with rapid eye movements were not recorded in sleep electroencephalograms. In January 2000, he died of pneumonia at the age of 52 years, about 27 months after the onset of disease.

Patient II-3, one of the brothers of Patient II-5, also showed rapidly progressive cerebellar ataxia. He developed an ataxic gait, forgetfulness and dysarthria at the age of 55 years. Brain computed tomography demonstrated moderate cerebellar atrophy, and electroencephalograms showed diffuse intermittent slow activities without periodic synchronous discharges. He developed myoclonic jerks, akinetic mutism with a decorticate posture, and died 7 months after the onset. Patient I-1, the father of Patients II-5 and II-3, had also developed an ataxic gait and dementia at the age of 55 years. He died of unknown causes after a clinical course of 12 months. Neither autopsy nor PRNP analysis was carried out in either Patient I-1 or Patient II-3. One of the children of Patient II-5 was revealed to have PRNP D178N-129Met mutation (homozygous for 129Met).

Materials and methods

Autopsy was performed 6 h *post-mortem*. A frontal tip of the right cerebral hemisphere and a cerebellar tip were sampled and frozen for Western blot analysis. The remaining brain was immersion-fixed in 10% formalin for 2 weeks. Tissue blocks were immersed in 98% formic acid for 1 h and paraffin-embedded. Hematoxylin and eosin (HE) stain, Klüver-Barrera stain and Bodian's method were performed on 7- μ m-thick sections. Immunohistochemical analyses were performed by a standard indirect method for glial fibrillary acidic protein (GFAP) (polyclonal, Dako, Denmark, or monoclonal, clone G-A-5, Roche, Switzerland), ferritin (polyclonal, Dako), β -amyloid precursor protein (APP) (monoclonal, clone LN27, Zymed, USA), SNAP-25 (monoclonal, clone MAB331, Chemicon, USA) and prion protein (PrP) (monoclonal, clone 3F4, Senetek, USA). For anti-PrP immunohistochemistry, sections were pretreated with hydrolytic autoclaving as previously reported [11]. Western blot analysis for protease-resistant PrP (PrP^{res}) was performed using frontal cortical and cerebellar tissue tips from this case, applying phosphotungstic acid precipitation of PrP^{res} as described previously [12] with 50 μ g/ml proteinase K (PK) digestion, along with a control case with sporadic

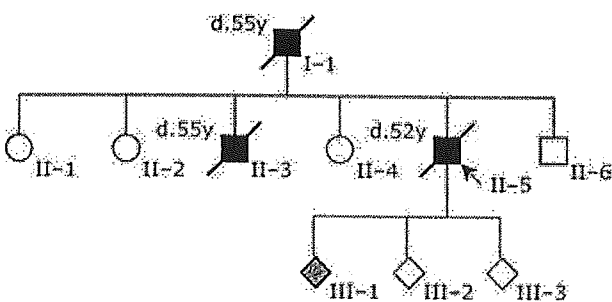


Figure 1. Family tree of the present pedigree. Patients who developed rapidly progressive cerebellar ataxia are depicted by closed symbols, along with their age at death (years old). One of the children of the present case has fatal familial insomnia genotype D178N-129Met/Met (grey symbol).

CJD (77-year-old man, duration of illness was 9 months, 129Met/Met). Transmission study was performed as described previously [13]. Briefly, frontal cortical tissue tips were aseptically homogenized with nine volumes of saline, and after removal of debris by low-speed centrifugation the supernatant was used as 10% homogenate. Twenty microliters of 10% homogenate were injected intracerebrally into female NZW mice or female Tg7 mice expressing hamster PrP but not endogenous murine PrP. Sections of infected mice were analysed by HE stain and also by immunohistochemistry for PrP (polyclonal, PrP-C, IBL, Japan) and GFAP (clone G-A-5, Roche). Permission for the animal experiments was obtained from the Animal Experiment Committee of Kyushu University.

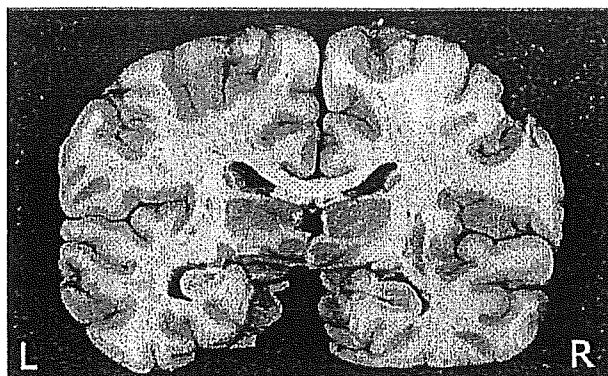


Figure 2. Coronal section at the thalamic level. The medial part of the thalamus is atrophic and the third ventricle is dilated.

Results

The brain weighed 1350 g before fixation. The cerebellum showed slight atrophy, whereas the volume of the forebrain was preserved. Coronal sections showed atrophy of the medial part of the thalamus and symmetrical dilatation of the third ventricle (Figure 2).

The summary of histological examination is shown in Figure 3. Marked neuronal loss and moderate astrogliosis in the thalamus were observed, most prominently in its centromedial nucleus and dorsomedial nucleus. However, spongiform change was imperceptible (Figure 4A,B). Neuronal loss and gliosis in the medial portion of the inferior olivary nucleus were also apparent (Figure 4C,D). In the cerebellum there was mild loss of granular cells, and the molecular layer was slightly atrophic. There were localized lesions of spongiosis in the cerebellar molecular layer. Purkinje's cells appeared not to be decreased in number, but they often demonstrated shrunken features. The cerebellar white matter showed diffuse myelin pallor. The cerebral cortex showed uneven distribution of spongiform change and neuronal loss (Figure 4E). There was no apparent difference in the intensities of the cortical lesions among the lobes of the cerebrum except that the lesions are more prominent in the entorhinal cortex and less in the occipital lobe. Moderate astrogliosis was associated with the spongiform lesions (Figure 4F).

Immunohistochemistry for PrP revealed that there was no punctate or plaque-type immunoreactivity in the thal-

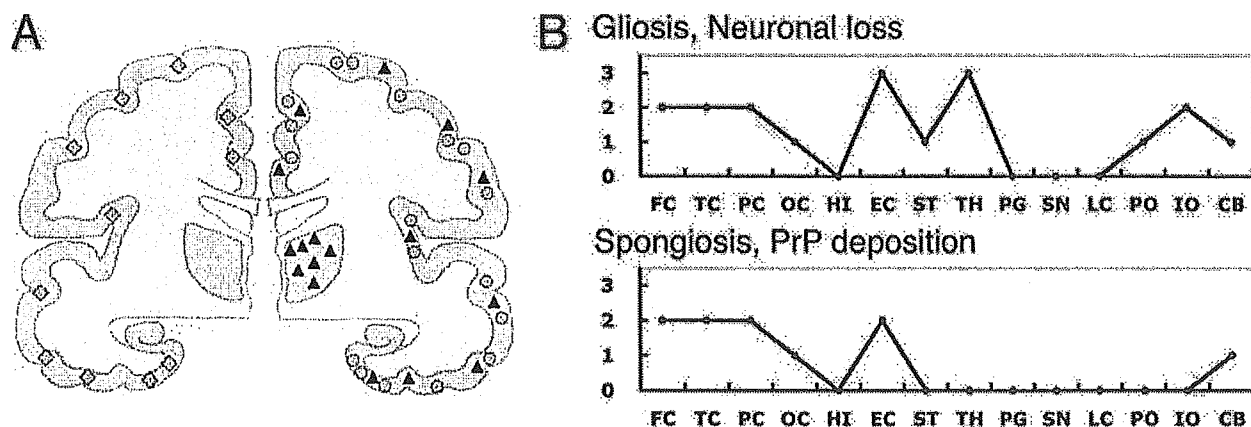


Figure 3. Lesion profiles of the present case. A: schematic drawing of the distribution of prion protein (PrP) deposition (diamonds), spongiosis (circles) and neuronal loss (triangles) in this case, which can be compared to that of fatal familial insomnia (FFI) and 178CJD shown in ref. [19]. B: lesion profiles in respect to gliosis/neuronal loss and spongiosis/PrP deposition. Brain regions studied were: frontal cortex (FC), temporal cortex (TC), parietal cortex (PC), occipital lobe (OC), hippocampus (HI), entorhinal cortex (EC), striatum (ST), thalamus (TH), substantia nigra (SN), periaqueductal grey (PG), pons (PO), locus ceruleus (LC), medulla oblongata (ME), cerebellum (CB). The vertical axis is the degree of lesion graded as follows. 0: not detectable; 1: mild; 2: moderate; 3: severe.

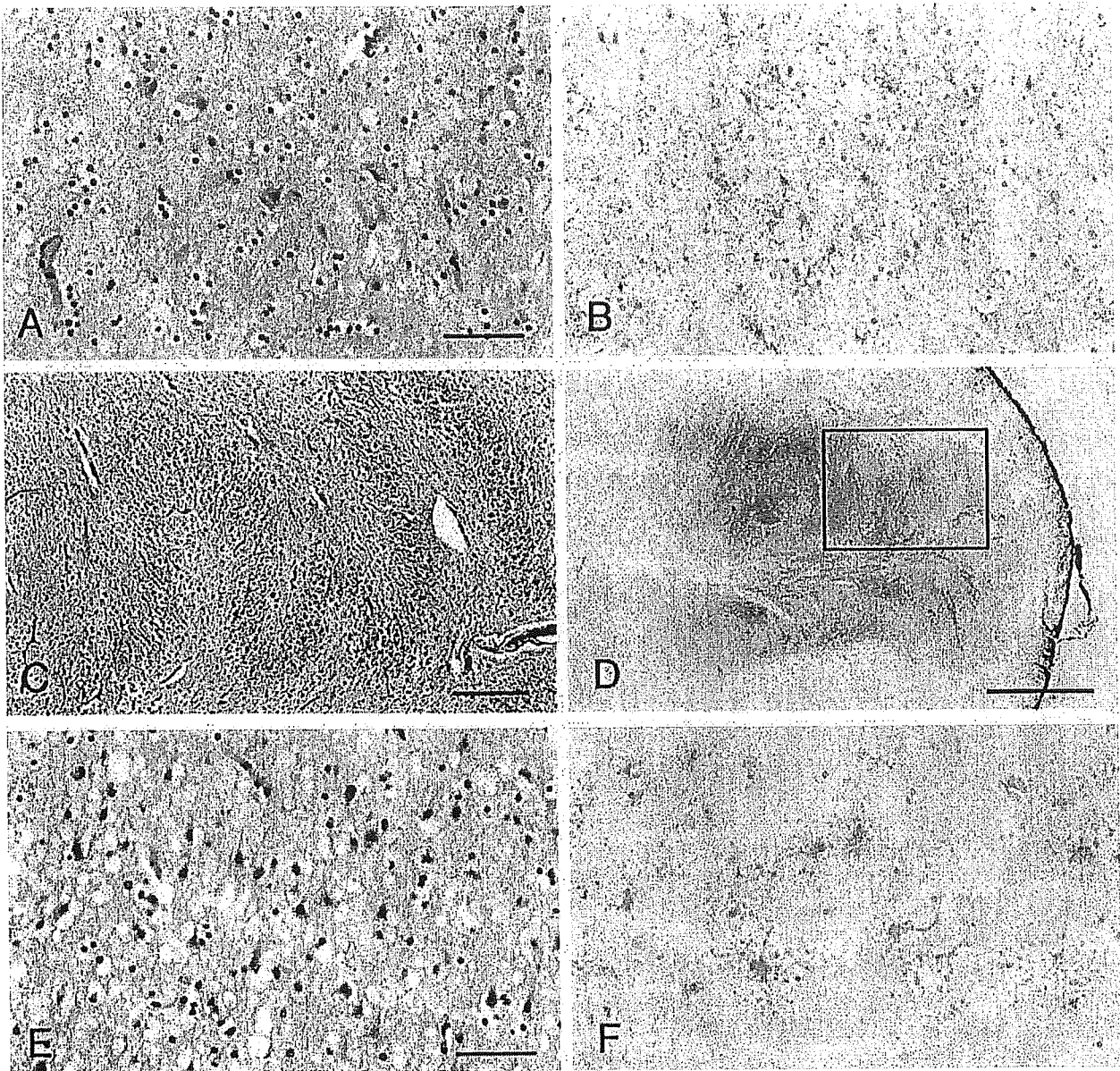


Figure 4. Neuronal loss and gliosis revealed by haematoxylin and eosin stain (A, E), Bodian's stain (C) or immunohistochemistry for glial fibrillary acidic protein (GFAP) (B, D, F). A, B: centromedial nucleus of the thalamus. C, D: inferior olivary nucleus. Neuronal loss is more evident in the medial part (left side of panel C, which represents the rectangular area depicted in panel D). E, F: cerebral cortex (frontal lobe). Both spongiform change and gliosis are remarkable. Bars: 50 μ m (A, B, E, F), 200 μ m (C), 1 mm (D).

amus or inferior olivary nucleus (Figure 5C,D). In the cerebellar molecular layer, punctate deposits of PrP were focally observed (Figure 5A), and the regions with these deposits were coincident with the extent of spongiform change. Likewise, fine granular deposition of PrP was also detected together with spongiform degeneration in the cerebral cortex (Figure 5B). The distribution of PrP deposits appeared to be more broad and noticeable in the cere-

bral cortex than in the cerebellum. As a unique finding, the anti-PrP antibody revealed swollen and/or frizzled axons in the deeper parts of the cerebral white matter, in the corpus callosum, or at the borders of the thalamus and caudate nucleus (Figure 5E). Axonal transported substances, APP (Figure 5E, inset) and SNAP-25 (data not shown) were also detected immunohistochemically in those axons.

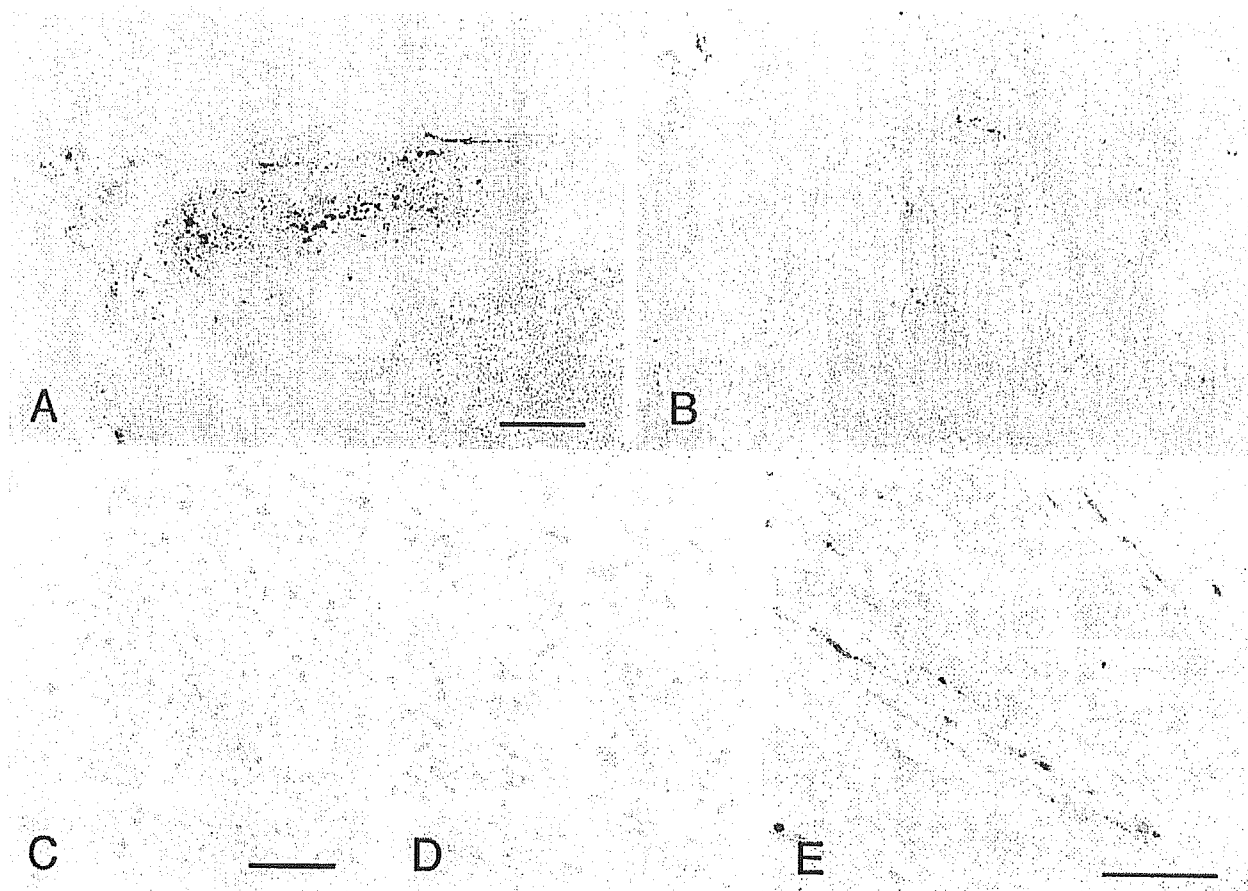


Figure 5. Immunohistochemistry for prion protein (PrP) deposition. A: cerebellum. B: frontal cortex. C: centromedial nucleus of the thalamus. D: inferior olivary nucleus. PrP deposition can not be detected in the thalamus or the inferior olivary nucleus, but coarse or fine granular PrP deposition is visible within the cerebral cortex and the cerebellar molecular layer. E: axons with swollen and/or frizzled features can be detected in the white matter at the border of the thalamus. These axons are also immunostained with anti-APP (amyloid precursor protein) antibody (inset). Bars: 50 μm (A, B, E), 100 μm (C, D).

Although the conventional method of Western blot analysis for PrP^{res} failed to detect any particular signal (data not shown), by application of phosphotungstic acid precipitation that preferably concentrates PrP^{res} but not cellular PrP [12], Western blot analysis of the extract from the frontal cortex of this case revealed a detectable amount of PrP^{res} (Figure 6). The molecular weight of non-glycosylated form of PrP was about 19 kDa (PrP^{res} type 2 pattern) and also the PrP^{res} glycoform ratio was compatible with that of FFI, which has been previously reported [14]. The extract from the cerebellum showed no significant signal in Western blot analysis even with phosphotungstic acid precipitation (data not shown).

The disease of this case was successfully transmitted to some of the mice inoculated with tissue homogenate from the frontal cortex. The incubation time was 571.6 ± 61.1

days (5/7 of the inoculated mice developed TSE) in the NZW mice and 736 ± 64.4 (5/8) in the Tg7 mice, respectively. Although not all the mice developed TSE, diseased mice demonstrated lethargy in the terminal stage rather than excitability. In the TSE-developed mice pathological examination of the brain showed that spongiform change and gliosis were prominent in the cerebral cortex in addition to the thalamus (Figure 7). Immunohistochemistry for PrP revealed that diffuse granular PrP deposition was present within the deep layer of the cerebral cortex as well as in the lateral portion of the thalamus (Figure 7B,E).

Discussion

It is established that there is an overlapping spectrum between classical FFI and CJD in association with PRNP

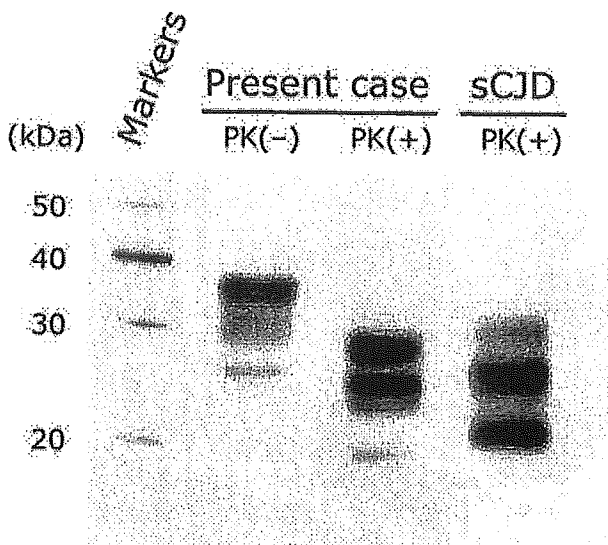


Figure 6. Western blot analysis for protease-resistant prion protein (PrP^{res}). Brain homogenate of the frontal cortex of this case is treated with or without proteinase K (PK), and then PK-digested sample is followed by the 40-times concentration with phosphotungstic acid precipitation for PrP^{res}. The abnormal PrP molecules in the frontal cortex of this case migrate as PrP^{res} type 2. PrP molecules in the lane sporadic Creutzfeldt-Jakob disease (sCJD) are also shown as a standard type 1 PrP (MM1). Molecular sizes (kDa) are indicated on the left.

D178N [6]; however, this case adds to our knowledge about this disease. Although the present case had FFI genotype, the clinical features were initially characterized by prominent cerebellar ataxia, and the neuropathological findings were also atypical in the following respects. First, PrP deposition and spongiform change in the cerebral cortex were more conspicuous than in the thalamus or inferior olivary nucleus, both of which are extremely vulnerable sites for FFI. It has been previously reported that heterozygotes Met/Val at codon 129 result in a longer clinical course than homozygotes [4], and it is therefore possible that the lesions seen in the cerebral cortex were more prominent simply because of the longer course of illness in this patient. However, a further noteworthy point about this case is rather that there was no PrP deposition either in the thalamus or in the inferior olivary nucleus.

Second, immunohistochemical examination detected a peculiar deposition of PrP within the molecular layer of the cerebellum. The localized lesions of granular deposits of PrP and spongiform change in the cerebellar molecular layer seemed to be similar to those reported in a patient from an Austrian FFI family [15]. The cerebellar ataxia of this case could have attributed to the loss of granular neu-

rones and degeneration of Purkinje's cells, in addition to the lesions of the inferior olivary nucleus, although the pathology related to PrP deposition could have also been responsible.

A third atypical feature is that the neuronal loss in the thalamus was most noticeable in the centromedial nucleus. A previous study revealed that severe atrophy of the anterior ventral and dorsomedial thalamic nuclei was consistently observed, whereas that of other thalamic nuclei was less severe and they were inconsistently affected [2]. In this case, the medial portion of the thalamus was indeed damaged crucially, but the principal lesion was different from the typical pathology of FFI.

In addition, an interruption of axonal transport was suggested. Some of the axons were swollen and associated with PrP accumulation, and both APP and SNAP-25 were also accumulated in those axons. APP and SNAP-25 are presynaptic protein and APP is considered as the most effective marker for axonal injury [16]. Aberration in recruitment of PrP might be involved in the pathogenesis of TSE, as described previously [17,18].

This case showed a small amount of specific PrP^{res} in the cerebral cortex but not in the cerebellum as detected by Western blotting. The ratio of PrP^{res} quantity in those regions was visually correlated with that of immunohistochemical reactivity for PrP. Although fresh frozen samples from the thalamus or the inferior olivary nucleus were not obtained for Western blot analyses, we suspect that PrP^{res} in such regions would be too sparse to be detected by Western blotting even in combination with phosphotungstic acid precipitation. The type 2 migration pattern and the glycoform ratio of PrP^{res} in this case were compatible with those in the typical FFI [14]; however, it remains to be elucidated whether these abnormal proteins that can be classified in the same PrP^{res} type may have different influences on the neurodegeneration processes.

Finally, the transmission study revealed that a pathogen in the frontal cortex of this case might be different from that of an FFI case previously reported by Dr Tateishi and his colleagues [13]. NZW mice infected with a thalamic tissue sample of a typical FFI case exhibited excitability as the principal clinical sign and demonstrated PrP deposition predominantly localized within the thalamus. On the other hand, NZW mice infected with a frontal cortical tissue sample from the present case showed lethargy as a clinical sign, and demonstrated diffuse PrP deposition within the deep layer of the cerebral cortex, as well as in the lateral portion of the thalamus. The PrP deposition

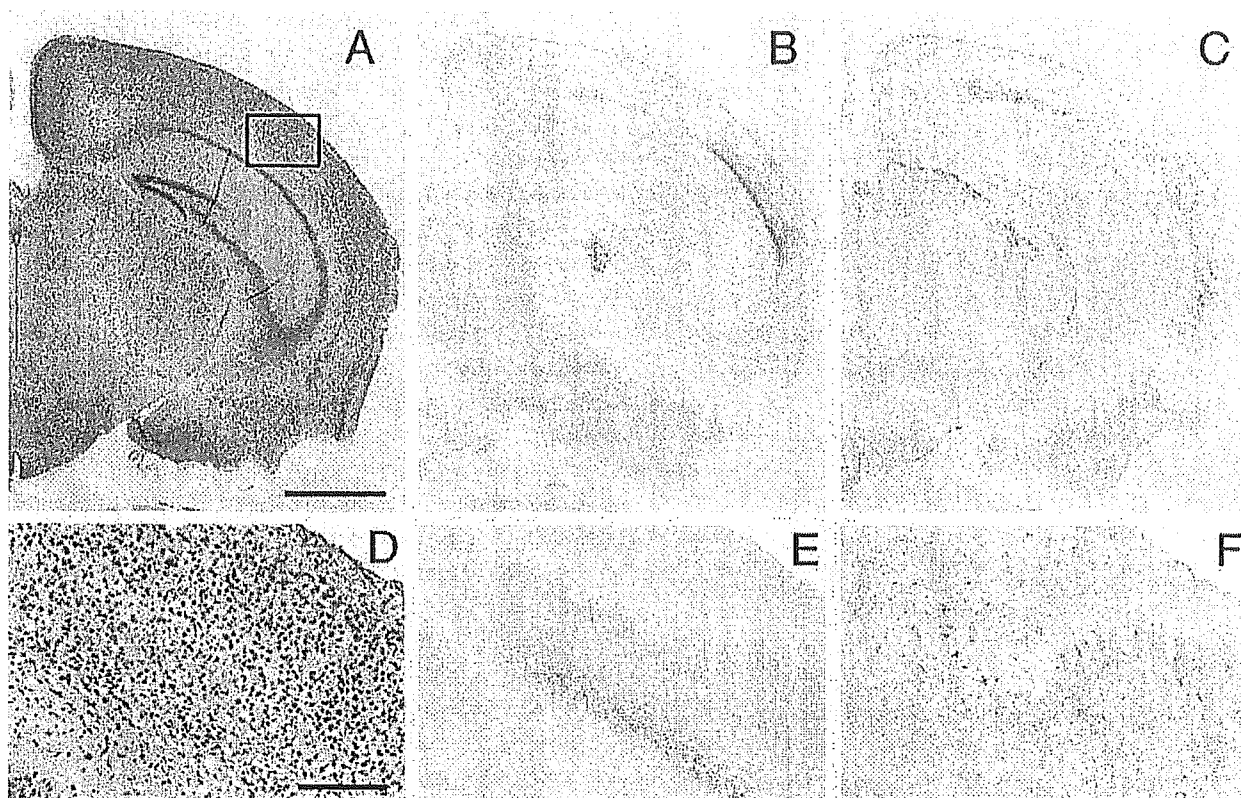


Figure 7. Histological profiles of the mice inoculated with the patient's brain material. A, D: hematoxylin and eosin stain. B, E: prion protein (PrP). C, F: glial fibrillary acidic protein. Spongiform change, PrP deposition and astrocytic gliosis can be observed within the deep layer of the cerebral cortex as well as in the lateral portion of the thalamus. D–F: high power magnifications of the cortical lesions represent the rectangular area depicted in panel A. Bars: 1 mm (A–C), 150 μ m (D–E).

pattern of this mouse was distinctive against that of mouse models with other scrapie strains, thus refuting the possibility of contamination. It is not clear whether there were more than two pathogen strains in the brain and whether the strains were dependent on the brain areas. Because we have not examined transmissibility of this case systematically and not obtained frozen materials for Western blot analysis, this aspect still awaits further clarification.

In conclusion, the present case which had FFI genotype showed atypical features, especially with regard to the PrP deposition pattern; there was no deposition within the thalamus or inferior olivary nucleus. Diversity in disease phenotype among patients with the same genotype suggests that some other unidentified factors as well as abnormal PrP deposits or other as yet unknown genetic factors may be responsible for the pathogenesis of the disease. In this study we have shown that variation in pathogen strains may also be one such factor and this factor could have greatly affected the pathogenesis in the present case of FFI.

Acknowledgements

We thank Ms K. Hatanaka for her excellent technical assistance. This study was supported partly by a grant to K. Doh-ura from the Ministry of Health, Labour and Welfare, Japan. Part of this study was carried out at the Morphology Core, Graduate School of Medical Sciences, Kyushu University. The English used in this manuscript was revised by Miss K. Miller (Royal English Language Centre, Fukuoka, Japan).

References

- 1 Goldfarb LG, Petersen RB, Tabaton M, Brown P, LeBlanc AC, Montagna P, Cortelli P, Julien J, Vital C, Pendelbury WW, Haltia M, Wills PR, Hauw JJ, McKeever PE, Monari L, Schrank B, Swergold GD, Gambetti LA, Gajdusek DC, Lugaresi E, Gambetti P. Fatal familial insomnia and familial Creutzfeldt-Jakob disease: disease phenotype determined by a DNA polymorphism. *Science* 1992; **258**: 806–8

- 2 Manetto V, Medori R, Cortelli P, Montagna P, Tinuper P, Baruzzi A, Rancurel G, Hauw JJ, Vanderhaeghen JJ, Maillieux P, Bugiani O, Tagliavini F, Bouras C, Rizzuto N, Lugaresi E, Gambetti P. Fatal familial insomnia: clinical and pathologic study of five new cases. *Neurology* 1992; 42: 312-9
- 3 Lugaresi E, Medori R, Montagna P, Baruzzi A, Cortelli P, Lugaresi A, Tinuper P, Zucconi M, Gambetti P. Fatal familial insomnia and dysautonomia with selective degeneration of thalamic nuclei. *N Engl J Med* 1986; 315: 997-1003
- 4 Parchi P, Petersen RB, Chen SG, Autilio-Gambetti L, Capellari S, Monari L, Cortelli P, Montagna P, Lugaresi E, Gambetti P. Molecular pathology of fatal familial insomnia. *Brain Pathol* 1998; 8: 539-48
- 5 McLean CA, Storey E, Gardner RJ, Tannenberg AE, Cervenakova L, Brown P. The D178N (cis-129M) 'fatal familial insomnia' mutation associated with diverse clinicopathologic phenotypes in an Australian kindred. *Neurology* 1997; 49: 552-8
- 6 Zerr I, Giese A, Windl O, Kropp S, Schulz-Schaeffer W, Riedemann C, Skworc K, Bodemer M, Kretzschmar HA, Poser S. Phenotypic variability in fatal familial insomnia (D178N-129M) genotype. *Neurology* 1998; 51: 1398-405
- 7 Nagayama M, Shinohara Y, Furukawa H, Kitamoto T. Fatal familial insomnia with a mutation at codon 178 of the prion protein gene: first report from Japan. *Neurology* 1996; 47: 1313-6
- 8 Kawasaki K, Wakabayashi K, Kawakami A, Higuchi M, Kitamoto T, Tsuji S, Takahashi H. Thalamic form of Creutzfeldt-Jakob disease or fatal insomnia? Report of a sporadic case with normal prion protein genotype. *Acta Neuropathol (Berl)* 1997; 93: 317-22
- 9 Mizusawa H, Ohkoshi N, Sasaki H, Kanazawa I, Nakanishi T. Degeneration of the thalamus and inferior olives associated with spongiform encephalopathy of the cerebral cortex. *Clin Neuropathol* 1988; 7: 81-6
- 10 Taniwaki Y, Hara H, Doh-Ura K, Murakami I, Tashiro H, Yamasaki T, Shigeto H, Arakawa K, Araki E, Yamada T, Iwaki T, Kira J. Familial Creutzfeldt-Jakob disease with D178N-129M mutation of PRNP presenting as cerebellar ataxia without insomnia. *J Neurol Neurosurg Psychiatry* 2000; 68: 388
- 11 Sasaki K, Doh-ura K, Ironside JW, Iwaki T. Increased clusterin (apolipoprotein J) expression in human and mouse brains infected with transmissible spongiform encephalopathies. *Acta Neuropathol (Berl)* 2002; 103: 199-208
- 12 Safar J, Wille H, Itri V, Groth D, Serban H, Torchia M, Cohen FE, Prusiner SB. Eight prion strains have PrP (Sc) molecules with different conformations. *Nat Med* 1998; 4: 1157-65
- 13 Tateishi J, Brown P, Kitamoto T, Hoque ZM, Roos R, Wollman R, Cervenakova L, Gajdusek DC. First experimental transmission of fatal familial insomnia. *Nature* 1995; 376: 434-5
- 14 Parchi P, Capellari S, Gambetti P. Intracerebral distribution of the abnormal isoform of the prion protein in sporadic Creutzfeldt-Jakob disease and fatal insomnia. *Microsc Res Tech* 2000; 50: 16-25
- 15 Almer G, Hainfellner JA, Brucke T, Jellinger K, Kleinert R, Bayer G, Windl O, Kretzschmar HA, Hill A, Sidle K, Collinge J, Budka H. Fatal familial insomnia: a new Austrian family. *Brain* 1999; 122: 5-16
- 16 Sherriff FE, Bridges LR, Gentleman SM, Sivaloganathan S, Wilson S. Markers of axonal injury in post mortem human brain. *Acta Neuropathol (Berl)* 1994; 88: 433-9
- 17 Ferrer I, Puig B, Blanco R, Marti E. Prion protein deposition and abnormal synaptic protein expression in the cerebellum in Creutzfeldt-Jakob disease. *Neuroscience* 2000; 97: 715-26
- 18 Liberski PP, Budka H. Neuroaxonal pathology in Creutzfeldt-Jakob disease. *Acta Neuropathol (Berl)* 1999; 97: 329-34
- 19 Montagna P, Gambetti P, Cortelli P, Lugaresi E. Familial and sporadic fatal insomnia. *Lancet Neurol* 2003; 2: 167-76

Received 4 February 2004

Accepted after revision 26 April 2004

Hidefumi Furuoka · Atushi Yabuzoe · Motohiro Horiuchi
Yuichi Tagawa · Takashi Yokoyama
Yoshio Yamakawa · Morikazu Shinagawa
Tetsutaro Sata

Effective antigen-retrieval method for immunohistochemical detection of abnormal isoform of prion proteins in animals

Received: 12 July 2004 / Revised: 12 October 2004 / Accepted: 12 October 2004 / Published online: 22 December 2004
© Springer-Verlag 2004

Abstract For immunohistochemistry of the prion diseases, several pretreatment methods to enhance the immunoreactivity of human and animal abnormal proteinase-resistant prion protein (PrP^{Sc}) on the tissue sections have been employed. The method of 121°C hydrated autoclaving pretreatment or the combination method of 121°C hydrated autoclaving with a certain chemical reagent (formic acid or proteinase K, etc) are now widely used. We found that an improved hydrated autoclaving method at 135°C, more effectively enhanced PrP^{Sc} immunoreactivity for the antibodies recognizing the linear epitope. In addition, this method was more effective for the long-term fixation samples as compared with other previous methods. However, this modified method could not retrieve PrP^{Sc} antigenic epitopes

composed of conformational structures or several discontinuous epitopes. We describe the comparative studies between our improved method and other antigen-retrieval procedures reported previously. Based on the differences of reaction among the antibodies, we also discuss the mechanisms of the hydrated autoclaving methods to retrieve PrP^{Sc} immunoreactivity.

Keywords Prion protein · Immunohistochemistry · Antigen retrieval · Autoclaving · Monoclonal antibody

H. Furuoka (✉) · A. Yabuzoe
Department of Pathobiological Science,
Obihiro University of Agriculture and Veterinary Medicine,
080-8555 Obihiro, Japan
E-mail: furuoka@obihiro.ac.jp
Fax: +81-155-495364

M. Horiuchi
Department of Applied Veterinary Science,
Obihiro University of Agriculture and Veterinary Medicine,
080-8555 Obihiro, Japan

M. Horiuchi
Research Center for Protozoan Diseases,
Obihiro University of Agriculture and Veterinary Medicine,
080-8555 Obihiro, Japan

Y. Tagawa · T. Yokoyama · M. Shinagawa
Prion Disease Research Center,
National Institute of Animal Health,
305-0856 Ibaraki, Japan

Y. Yamakawa
Department of Biochemistry and Cell Biology,
National Institute of Infectious Diseases,
162-8640 Tokyo, Japan

T. Sata
Department of Pathology,
National Institute of Infectious Diseases,
162-8640 Tokyo, Japan

Introduction

Scrapie in sheep and goat, bovine spongiform encephalopathy (BSE), chronic wasting disease in deer and Creutzfeldt-Jakob disease (sporadic, iatrogenic, familial and variant forms) and Kuru in humans are transmissible neurodegenerative disorders belonging to a group of prion diseases. They are characterized by the accumulation of abnormal proteinase-resistant prion protein (PrP^{Sc}), which is an isoform of the cellular, proteinase-sensitive prion protein (PrP^C), as a result of post-translational modification with increases of the population of β -sheet conformation in the brain [20]. The pathology is characterized by neuronal cell loss, spongiform change, gliosis and deposition of abnormal amyloid protein.

Immunohistochemistry to demonstrate PrP^{Sc} in tissue sections is now a well-established technique for the diagnosis of prion diseases [2]. It has been reported that PrP^{Sc} immunoreactivity is enhanced by several antigen-retrieval procedures such as formic acid [4, 10], a combination of formic acid pretreatment and microwave processing [7, 14], hydrated or hydrolytic autoclaving [6, 11], guanidine thiocyanate [4, 19], and combined protocols [1, 8, 9, 15].

The recent disclosure of BSE in Japan has started an active surveillance for all slaughter cattle since October 2001. Briefly, diagnostic procedure is follows: samples

have been taken from the medulla oblongata (obex region) and examined by ELISA as the primary screening test; the ELISA-positive samples have then been confirmed by Western blot and/or immunohistochemistry. In starting an active surveillance for BSE in Japan, we applied various pretreatment methods for different antibodies to formalin-fixed and paraffin-embedded tissues to enhance PrP^{Sc} immunoreactivity. Although the pretreatment methods reported previously were found to retrieve PrP^{Sc} for antibodies used in this study, we found that an improved hydrated autoclaving method at 135°C more effectively enhanced PrP^{Sc} immunoreactivity for the antibodies recognizing the linear epitope. However, our modified method could not retrieve PrP^{Sc} antigens well for the monoclonal antibodies recognizing the conformational structures.

Here we describe the comparative studies between our improved method and other antigen-retrieval procedures reported previously, and discuss the mechanisms of the hydrated autoclaving methods to retrieve PrP^{Sc} immunoreactivity.

Materials and methods

Samples

We used the brain tissues that were cut coronally at the level including hippocampus and thalamus from two scrapie-infected and two negative control ICR mice, the medulla oblongata at the level of the obex, and the spinal cord from three scrapie-affected and two negative control sheep, and from three BSE-affected cattle in Japan and two control cattle. Two mice were inoculated intracerebrally with scrapie G1 strain, which induces amyloid plaque formations in the brain. Affected or non-affected sheep and cattle were diagnosed and confirmed by histological, immunohistochemical, and Western blot methods. These samples were fixed in 15% formalin for 48–72 h and embedded routinely in paraffin. BSE tissue blocks were treated with 98% formic acid for 1 h to reduce the infectivity of prion after formalin fixation. In

addition, we prepared the serial tissue blocks from the medulla oblongata of scrapie-affected sheep, which was immersed in 15% formalin at least for 6 months.

Immunohistochemistry

Serial tissue sections, 4 µm in thickness, were picked up on silane-coated glass slides (Muto Purechemicals Co., Japan). After deparaffinization, endogenous peroxidase was blocked by incubation in 3% H₂O₂ for 5 min. We applied six different pretreatment protocols as follows: (1) 98% formic acid for 5 min (designated as FA); (2) hydrated autoclaving at 121°C, 2 atmosphere (atm) for 20 min (with Tomy high-pressure steam sterilizer KS-323, Japan) in distilled water (121DWHA); (3) 121DWHA and 98% formic acid for 5 min (121DWHA/FA); (4) 121DWHA and proteinase K (0.4 mg/ml, Dako, USA) treatment for 1 min (121DWHA/PK); (5) hydrated autoclaving at 135°C, 3 atm for 20 min in distilled water (135DWHA); (6) 135DWHA and 98% formic acid for 5 min (135DWHA/FA). After applying each pretreatment, tissue sections were incubated with 10% goat or horse normal serum (Nichirei, Japan) for 30 min. In this study, we used the avidin-biotin complex methods (ABC kit; Vector Lab., USA) and the horseradish peroxidase-labeled polymer methods (Envision+ kit; Dako). Sections were exposed to primary antibodies for overnight at 4°C or 1 h at room temperature for ABC kit or Envision+ kit, respectively. As negative controls, the sections were exposed for each primary antibody without any pretreatments. The following steps were performed with second antibodies and others according to the each manufacture's instructions. The signals were detected using diaminobenzidine (Simple stain DAB; Nichirei, Japan). Sections were counterstained with Mayer's hematoxylin.

The characteristics of the nine primary antibodies used in this study are summarized in Table 1. For sections prepared from the tissue blocks immersed in 15% formalin for 6 months, we tested the 121DWHA and 135DWHA methods using B103 and 43C5 antibodies.

Table 1 Characteristics of the nine antibodies used in this study (L linear epitope, DC discontinuous epitope, mAb monoclonal antibody, pAb polyclonal antibody)

Antibodies	Epitope		Clonality	Dilution	Immunogen	Source
	Position	L/DC				
132	119–127	L	mAb	1:200	Mouse recPrP	Horiuchi
149	147–153	L	mAb	1:500	Mouse recPrP	Horiuchi
43C5	163–169	L	mAb	1:10000	Mouse recPrP	Horiuchi
B103	103–121	L	pAb	1:1000	Cow recPrP	Horiuchi
6H4	155–163	L	mAb	1:500	Cow recPrP	Prionics (Zürich, Switzerland)
72	89–231(143–151)	DC	mAb	1:500	Mouse recPrP	Horiuchi
44B1	155–231	DC	mAb	1:200	Mouse recPrP	Horiuchi
44B2	155–231	DC	mAb	1:200	Mouse recPrP	Horiuchi
T2	Unknown	DC	mAb	1:500	Mouse recPrP	Tagawa

Morphometry

Serial sections from BSE-affected samples were pretreated with 121DWHA, 121DWHA/FA, 121DWHA/PK, 135DWHA, and 135DWHA/FA methods, and immunostained with four antibodies (B103, 43C5, 44B1, and 6H4), respectively. Each of the pretreatment conditions were evaluated on the selected five areas (total μm^2). The Lumina Vision computer analysis system (Mitani Corp., Tokyo, Japan) was used to measure the positive area of PrP immunostaining. The brown-colored chromogen precipitate was selected, digitized images of these areas, and the digital pixels converted into the density area (μm^2) on the software. The highest density measurement was set to 100% and relative density (RD) of immunostaining by the other pretreatments in the same area was calculated.

Results

Histopathology

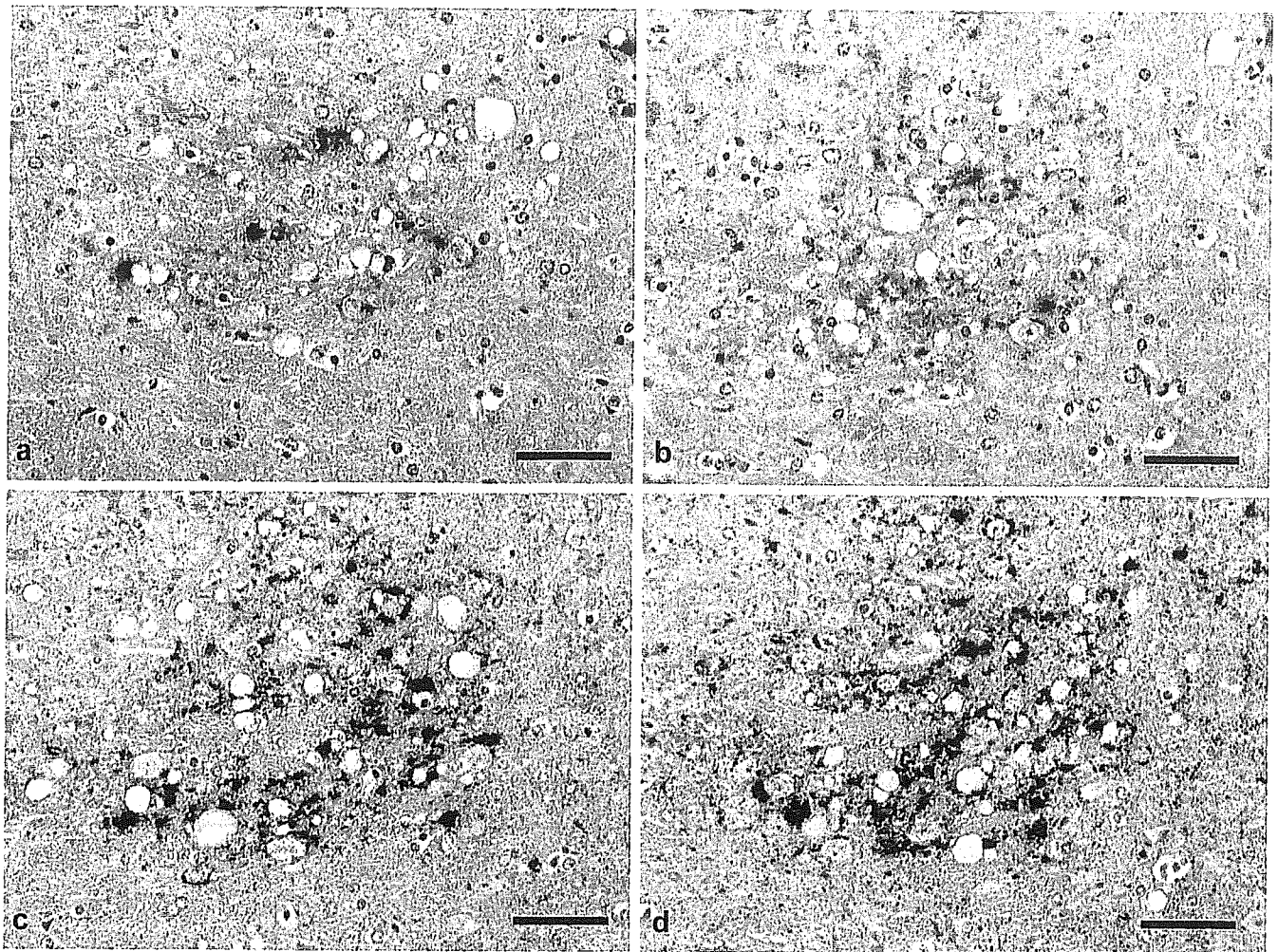
In the mouse, neuropil vacuolation associated with astrogliosis and microglial proliferation was observed throughout all areas of the brain. Amyloid plaque structures were also seen, which were often observed in contact with the capillary vessels.

In the obex region of scrapie-infected sheep, neuropil vacuolation and single or multiple intracytoplasmic vacuoles were particularly found in the dorsal motor nucleus of vagus nerve (DMNV), gracile nucleus, nucleus ambiguus and reticular formation [22]. The hypoglossal nucleus, olivary nucleus and nucleus of solitary tract (NST) were only mildly affected. In addition, spongiform

Table 2 Results of the immunoreactivity for the antibodies under pretreatment methods [FA 96% formic acid for 5 min, 121DWHA hydrated autoclaving at 121°C, 2 atmosphere (atm) for 20 min in distilled water, 121DWHA/FA 121DWHA and 96% formic acid for 5 min, 121DWHA/PK 121DWHA and proteinase K treatment for 1 min, 135DWHA hydrated autoclaving at 135°C, 3 atm for

20 min in distilled water, 135DWHA/FA 135DWHA and 98% formic acid for 5 min, M scrapie-affected mouse, C BSE-affected cow, S scrapie-affected sheep, P plaque type, D diffuse type, 3+ strongly positive signal, 2+ moderately positive signal, + faint positive signal, - negative]

Antibodies	Tissue source	Pretreatment					
		FA	121DWHA	121DWHA/FA	121DWHA/PK	135DWHA	135DWHA/FA
132	M/P	-	2+	2+	+	2+	2+
	M/D	-	+	2+	-	+	2+
	C	-	-	+	-	3+	3+
	S	-	-	2+	-	2+	3+
149	M/P	2+	+	2+	2+	3+	2+
	M/D	+	+	2+	+	3+	+
	C	-	-	2+	-	+	3+
	S	-	+	2+	2+	2+	3+
43C5	M/P	+	2+	2+	2+	3+	3+
	M/D	-	2+	2+	2+	2+	2+
	C	-	2+	2+	2+	2+	3+
	S	-	2+	2+	2+	3+	3+
B103	M/P	-	+	2+	2+	3+	3+
	M/D	-	+	2+	2+	3+	3+
	C	-	+	2+	2+	3+	3+
	S	-	+	2+	2+	3+	3+
6H4	M/D	-	+	2+	+	-	-
	M/P	-	+	2+	-	-	-
	C	-	+	2+	-	-	-
	S	-	+	2+	-	-	-
72	M/P	2+	+	3+	-	-	2+
	M/D	-	-	+	-	-	-
	C	+	-	2+	+	-	-
	S	-	+	2+	-	-	-
44B1	M/P	+	+	2+	-	+	2+
	M/D	-	-	2+	-	-	2+
	C	+	+	2+	-	-	+
	S	-	-	2+	-	-	+
44B2	M/P	+	+	3+	-	-	2+
	M/D	-	-	2+	-	-	+
	C	-	-	2+	-	-	-
	S	-	-	2+	-	-	-
T2	M/P	2+	+	3+	-	-	+
	M/D	-	-	2+	-	-	-
	C	-	-	2+	-	-	+
	S	-	-	2+	-	-	-



Bar: 50 μ m

Fig. 1 Immunohistochemistry of the PrP with mAb 43C5 in the thalamus of scrapie-affected mouse; **a** 121DWHA, **b** 121DWHA/FA, **c** 135DWHA and **d** 135DWHA/FA methods. The immunodensity is considerably greater using the 135DWHA and 135DWHA/FA methods [*PrP* prion protein, 121DWHA hydrated autoclaving at 121°C, 2 atmosphere (atm) for 20 min in distilled water, 121DWHA/FA 121DWHA and 96% formic acid for 5 min, 135DWHA hydrated autoclaving at 135°C, 3 atm for 20 min in distilled water, 135DWHA/FA 135DWHA and 98% formic acid for 5 min]. Bars **a-d** 50 μ m

neuropil lesions were seen in the periphery of the dorsal column of spinal cord and the vertebral column.

In BSE cases, because of the subclinical case, extremely mild spongiform lesions were observed only in the DMNV, and periphery of the reticular formation [24].

Immunohistochemistry

Immunohistochemical examination revealed that no PrP depositions were observed in the sections from the affected animals without pretreatment and from the control animals with and without pretreatment.

PrP^{Sc} immunostaining yielded characteristic patterns in each animals affected with prion disease [21]. The following immunostaining patterns were observed: (1) fine particulate deposition; (2) coarse particulate deposition; (3) perineuronal deposition; (4) glial type deposition; (5) perivascular or perivacuolar deposition; (6) plaque or plaque-like deposition.

In scrapie-infected mice, PrP^{Sc} deposits were observed diffusely in cortex, thalamus, and hippocampus. Perivascular, perivacuolar PrP^{Sc} deposits and plaque or plaque-like structures in thalamus were also seen.

The PrP^{Sc} deposits in scrapie-affected sheep were most intense in the DMNV. The hypoglossal nucleus also showed deposits, but the staining was sparse. Glial, coarse particulate, perineuronal, perivascular and perivacuolar depositions were found in the reticular formation.

In BSE cases, the intense positive reactions of PrP^{Sc} were observed in the DMNV, NST and periphery of the reticular formation, which showed fine, perineuronal and perivacuolar patterns. Fine or coarse particulate depositions were seen in olivary nucleus. The hypoglossal nucleus also showed positive reactions, but with a low intensity of immunostaining.